Buckling Coefficients for Fiber-Reinforced Plastic-Faced Sandwich Plates Under Combined Loading

Koganti Mohana Rao*
Indian Institute of Technology, Kharagpur, India

The buckling coefficients of rectangular anisotropic sandwich panels faced with fiber-reinforced plastic when under combined loading are evaluated by the Rayleigh-Ritz method. The results show that: 1) the presence of low in-plane positive shear k_s increases the axial buckling strength k_x of the panel; 2) over the range of values of aspect ratio λ, normal compression k_y, and in-plane shear k_s considered, the fiber orientation angle θ at which the buckling load N_{0x} is maximum varies between 0–65 deg; 3) the rate of decrease of k_x with k_y is greater at larger values of k_y; 4) positive shear (say $k_s = +2$) reduces k_x less than numerically equal negative shear ($k_s = -2$); and 5) for core-to-face thickness ratios t_c/t_f less than about 70, the buckling coefficient k_x is greater in the presence of larger positive shear than that in the presence of certain values of numerically smaller negative shear, e.g., k_x is larger at $k_y = 1$ and $k_s = +8$ than at $k_y = 1$ and $k_s = -2$ for $t_c/t_f < 65$.

Nomenclature

a, b	= length and width of plate, see Fig. 1
A	= column vector of A_{mn}, Eq. (12)
A_{mn}, B_{mn}, C_{mn}	= undetermined coefficients of trial solution
D_{ij} $(i, j = 1,2,3)$	= flexural stiffness, Eq. (3)
D_1, D_2, D_3, D_4, D_5	$= (D_{12}, D_{22}, D_{33}, D_{13}, D_{23})/D_{11}$, Eq. (10)
E_1, E_2	= longitudinal and transverse elastic moduli of face
G_{xz}, G_{yz}	= transverse shear moduli of core
G_{12}	= in-plane shear modulus of face
h_k	= normal distance of the inner surface of kth layer measured from xy plane
J_x, J_y	$= (S_x, S_y)b^2/\pi^2 D_{11}$, Eq. (10)
k_x, k_y, k_s	= normalized values of N_{0x}, N_{0y}, and N_{xy}, Eq. (10)
m, n, p, q	= half-wavelength integers
M	$= (m^2 - p^2)(n^2 - q^2)$
M_x, M_y, M_{xy}	= stress couples per unit length
N	= number of layers in each face
N_x, N_y, N_{xy}	= in-plane external forces per unit length
N_{0x}, N_{0y}	= maximum external normal compressions in x and y directions, respectively
P, Q	= symmetric real matrices, Eq. (11)
Q_x, Q_y	= transverse shear forces per unit length, see Fig. 1
$\bar{Q}^k_{ij}(i, j = 1,2,3)$	= transformed reduced stiffnesses of kth layer
S_x, S_y	= shear stiffnesses of core per unit length, Eq. (2)
t_c, t_f	= core and face thicknesses, respectively,
V	= potential energy
w	= deflection of plates
x, y, z	= Cartesian coordinates
$( ), x, y$	= derivatives with respect to x and y
X_{mn}, Y_{mn}	$= (B_{mn}/S_x, C_{mn}/S_y)b$
α_m, β_n	$= (m/a, n/b)\pi$
γ_x, γ_y	= bending load coefficient, see Fig. 1a
λ	$= a/b$
μ_{12}	= Poisson's ratio of face

Received Feb. 10, 1986; revision received Aug. 6, 1986.

*Assistant Professor, Mechanical Engineering Department.

HIGH-SPEED military aircraft and space vehicles demand the locational and directional distribution of stress in their structural members for optimum performance. The directional and locational distribution of the stress is achieved by sandwich construction with faces made of fiber-reinforced plastic (FRP) composites. Very careful analysis of such sandwich construction is required because of its direction- and location-dependent mechanical characteristics. In such applications as the panels of aircraft wing skins where the loading is of a combined nature, the analysis is further complicated.

One can find many analyses of isotropic sandwich plates in the literature. However, the analysis of anisotropic FRP-faced sandwich plates is limited. The available analyses were done with such simplifying assumptions as laminated faces that were effectively orthotropic (i.e., the coupling between stretching and shearing is neglected), were thin, etc. Libove and Batdorf[1] presented a general small-deflection theory for orthotropic flat sandwich plates. Robinson[2] used the theory of Libove and Batdorf for the buckling and bending analyses of orthotropic sandwich panels. Experimental studies of the four basic failures (general buckling, face wrinkling, shear crimping, and face dimpling of fiberglass) reinforced facing sandwich structures were carried out by Nordby and Crisman.[3] Theoretical and experimental analyses to determine the overall buckling and face-plate wrinkling loads of orthotropic sandwich panels with carbon fiber-reinforced plastic faces and honeycomb core subjected to uniaxial compression were reported in Refs. 4 and 14. Gutierrez and Webber[5] developed a theory and applied it to the determination of face wrinkling in honeycomb sandwich beams with laminated faces.

In the above references, the sandwich structures are treated as specially orthotropic, i.e., the geometric axes are parallel to the principal material directions. There are only limited references on the analysis of generally orthotropic sandwich panels (i.e., those having geometric axes and principal material directions inclined toward each other). Stroud and Kingsbury[6] dealt with the determination of stresses and deformations in a generally orthotropic sandwich plate under a uniform lateral load. Koganti and Kaeser[7] and Koganti[8] modified the general small-deflection theory of orthotropic sandwich plates outlined in Ref. 1 to suit to the analysis of a generally orthotropic (anisotropic) plate. The modified theory was then used to determine the buckling loads of FRP-faced anisotropic sandwich panels under axial compression and shear. Koganti[9] derived the force-deformation relations of cylindrically curved symmetric anisotropic sandwich plate using Castigliono's theorem of minimum complementary energy. With these relations, the Rayleigh-Ritz method was applied to the buckling analysis of FRP-faced curved sandwich panels under combined axial and bending loads.

Kuenzi[12] applied the energy method to obtain the buckling coefficients of orthotropic sandwich panels subjected to biaxial compression. The elastic bending and buckling of initially warped isotropic panels under combined loading was investigated by Chang and Fang.[11] Harris and Auelmann[10] discussed the stability of simply supported corrugated core sandwich plates under combined loading.

The analytical procedure of Refs. 7 and 8 is extended in the present paper to determine the buckling coefficients of simply supported FRP-faced rectangular sandwich panels under the combined action of biaxial compression, in-plane bending, and shear. The faces are built to be balanced, generally orthotropic, and thin in comparison to the core. The core is thick, specially orthotropic, and flexible in the plane of the plate. Under these conditions, the faces behave as membranes and the core resists only transverse shear forces. The geometry, the internal and external forces, and their sign conventions are shown in Fig. 1.

Formulation

The force displacement relations[8] of a balanced anisotropic sandwich panel are

$$\begin{Bmatrix} M_x \\ M_y \\ M_{xy} \end{Bmatrix} = - \begin{bmatrix} D_{11} & D_{12} & D_{13} \\ D_{12} & D_{22} & D_{23} \\ D_{13} & D_{23} & D_{33} \end{bmatrix} \times \begin{Bmatrix} w_{,xx} - Q_{x,x}/S_x \\ W_{,yy} - Q_{y,y}S_y \\ 2w_{,xy} - Q_{x,y}/S_x - Q_{y,x}/S_y \end{Bmatrix} \tag{1}$$

where M_x, M_y, and M_{xy} are the stress couples, Q_x and Q_y the transverse shear forces, S_x and S_y the transverse shear stiffnesses of core defined by

$$S_x = G_{xz} t_c \qquad S_y = G_{yz} t_c \tag{2}$$

and D_{ij} flexural stiffness coefficients of the sandwich plate defined by

$$D_{ij} = \frac{(t_c + t_f)^2}{2} \sum_{k=1}^{N} \bar{Q}_{ij}^k (h_{k-1} - h_k) \tag{3}$$

In Eqs. (2) and (3), G_{xz} and G_{yz} are the transverse shear moduli, t_c and t_f the thicknesses of the core and each face, h_k the distance of the inner surface of the kth layer measured from the xy plane, $\bar{Q}_{ij}^k$ the transformed reduced stiffnesses of the kth layer expressed[13] in terms of its principal material properties and fiber orientation angle θ, and N the number of layers in each face.

The edges of the plate are simply supported. They are also provided with stiffners such that transverse shear deformation is prevented in the cross-sectional plane. The boundary conditions are

$$w = M_x = Q_y = 0 \qquad \text{at } x = 0 \quad \text{and } a$$

$$w = M_y = Q_x = 0 \qquad \text{at } y = 0 \quad \text{and } b \tag{4}$$

where a and b are length and width of the plate (Fig. 1).

The buckling coefficients are evaluated by a Rayleigh-Ritz method that involves minimization of the potential energy. The trial solution needed for this method that satisfies the geometric boundary conditions of Eq. (4) are

$$w = \sum_{m=1}^{\infty} \sum_{n=1}^{\infty} A_{mn} \sin\alpha_m \times \sin\beta_n y \tag{5a}$$

$$Q_x = \sum_{m=1}^{\infty} \sum_{n=1}^{\infty} B_{mn} \cos\alpha_m \times \sin\beta_n y, \tag{5b}$$

$$Q_y = \sum_{m=1}^{\infty} \sum_{n=1}^{\infty} C_{mn} \sin\alpha_m \times \cos\beta_n y \tag{5c}$$

where m and n are half-wave integers and A_{mn}, B_{mn}, and C_{mn} undetermined coefficients. Also,

$$\alpha_m = m\pi/a, \qquad \beta_n = n\pi/b \tag{6}$$

Table 1 Values of D_{11} ($t_0/t_f = 20$ and $t_f = 0.315$ mm)

Fiber orientation θ, deg	$D_{11} \times 10^{-6}$, Pa	Fiber orientation θ, deg	$D_{11} \times 10^{-6}$, Pa
0	0.17127	45	0.07576
10	0.16386	60	0.04982
20	0.14371	70	0.04195
30	0.11624	80	0.03904
40	0.08817	90	0.03843

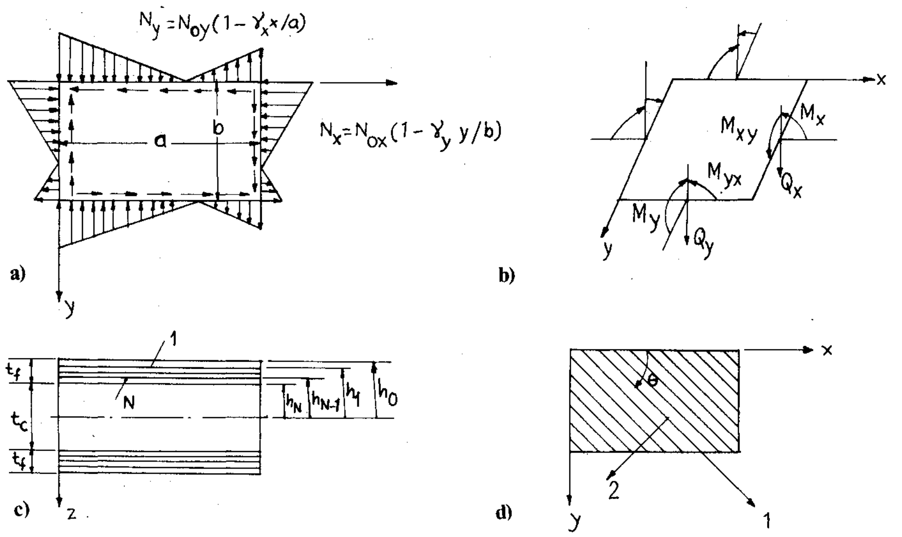

Fig. 1 Geometry and loading.

The total potential energy, V of the panel is the sum of the strain and potential energies of external forces N_x, N_y, and N_{xy} (see Fig. 1). Minimization of the potential energy V

$$V=\frac{ab}{8}\sum_{m=1}^{\infty}\sum_{n=1}^{\infty}\left[D_{11}\left(\frac{A_{mn}\alpha_m^2-B_{mn}\alpha_m}{S_x}\right)^2+D_{22}\left(\frac{A_{mn}\beta_n^2-C_{mn}\beta_n}{S_y}\right)^2+D_{33}\left(\frac{2A_{mn}\alpha_m\beta_n-B_{mn}\beta_n}{S_x}-\frac{C_{mn}\alpha_m}{S_y}\right)^2\right.$$

$$+2D_{12}\left(\frac{A_{mn}\alpha_m^2-B_{mn}\alpha_m}{S_x}\right)\left(\frac{A_{mn}\beta_n^2-C_{mn}\beta_n}{S_y}\right)-\frac{32}{\pi^2}\sum_{p=1}^{\infty}\sum_{q=1}^{\infty}\left\langle D_{23}\left(\frac{A_{mn}\beta_n^2-C_{mn}\beta_n}{S_y}\right)+D_{13}\left(\frac{A_{mn}\alpha_m^2-B_{mn}\alpha_m}{S_x}\right)\right\rangle$$

$$\times\left(2A_{pq}\alpha_p\beta_q-\frac{B_{pq}\beta_q}{S_x}-\frac{C_{pq}\alpha_p}{S_y}\right)\frac{mn}{M}+\frac{B_{mn}^2}{S_x}+\frac{C_{mn}^2}{S_y}-N_{0x}\alpha_m^2\left\langle A_{mn}^2-\frac{2\gamma_y}{b}A_{mn}\left(\frac{bA_{mn}}{4}-\frac{4b}{\pi^2}\sum_{q=1}^{\infty}\frac{nq}{(n^2-q^2)^2}A_{mq}\right)\right\rangle$$

$$\left.-N_{0y}\beta_n^2\left\langle A_{mn}^2-\frac{2\gamma_x}{a}A_{mn}\left(\frac{aA_{mn}}{4}-\frac{4a}{\pi^2}\sum_{p=1}^{\infty}\frac{m_p}{(m^2-p^2)^2}A_{pn}\right)\right\rangle+\frac{32N_{xy}}{ab}\sum_{p=1}^{\infty}\sum_{q=1}^{\infty}\frac{mnpq}{M}A_{mn}A_{pq}\right]$$

with respect to the undetermined coefficients A_{mn}, B_{mn}, and C_{mn}, yields the following three recurring equations:

1) $\dfrac{\partial V}{\partial A_{mn}}=0$:

$$\pi\left(m^4+D_2\lambda^4n^4+4D_3\lambda^2m^2n^2+2D_1\lambda^2m^2n^2\right)\frac{A_{mn}}{\lambda}-\left(m^3+2D_3\lambda^2mn^2+D_1\lambda^2mn^2\right)X_{mn}-\left(D_2\lambda^2n^2+2D_3m^2+D_1m^2\right)\lambda nY_{mn}$$

$$-32\sum_{p=1}^{\infty}\sum_{q=1}^{\infty}\times\left(D_5\lambda^2n^2+D_5\lambda^2q^2+D_4m^2+D_4p^2\right)\frac{mnpqA_{pq}}{\pi M}+16\sum_{p=1}^{\infty}\sum_{q=1}^{\infty}\left(D_5\lambda^2n^2+D_4m^2+2D_4p^2\right)\frac{\lambda mnqX_{pq}}{\pi^2M}$$

$$+16\sum_{p=1}^{\infty}\sum_{q=1}^{\infty}\left(D_5\lambda^2n^2+2D_5\lambda^2q^2+D_4m^2\right)\frac{mnpY_{pq}}{\pi^2M}-\pi\lambda^3k_y\left(1-\frac{\gamma_x}{2}\right)n^2A_{mn}-8\lambda^3k_y\gamma_x\sum_{p=1}^{\infty}\frac{mn^2pA_{pn}}{\pi(m^2-p^2)^2}$$

$$+32\lambda^2k_s\sum_{p=1}^{\infty}\sum_{q=1}^{\infty}\frac{mnpqA_{pq}}{\pi M}=\pi\lambda k_x\left(1-\frac{\gamma_y}{2}\right)m^2A_{mn}+8\lambda k_x\gamma_y\sum_{q=1}^{\infty}\frac{m^2nqA_{mq}}{\pi(n^2-q^2)^2}\tag{7}$$

2) $\dfrac{\partial V}{\partial B_{mn}}=0$:

$$\left(m^3+2D_3\lambda^2mn^2+D_1\lambda^2mn^2\right)A_{mn}-\left(\lambda m^2+D_3\lambda^3n^2+J_x\lambda^3\right)\frac{X_{mn}}{\pi}-\frac{(D_1+D_3)\lambda^2mnY_{mn}}{\pi}$$

$$-16\sum_{p=1}^{\infty}\sum_{q=1}^{\infty}\left(D_5\lambda^2npq^3+2D_4m^2npq+D_4np^3q\right)\frac{\lambda A_{pq}}{\pi^2M}+16\sum_{p=1}^{\infty}\sum_{q=1}^{\infty}\frac{D_4(m^2+p^2)\lambda^2nqX_{pq}}{\pi^3M}$$

$$+16\sum_{p=1}^{\infty}\sum_{q=1}^{\infty}\frac{\left(D_5\lambda^3npq^2+D_4\lambda m^2np\right)Y_{pq}}{\pi^3M}=0\tag{8}$$

3) $\dfrac{\partial V}{\partial C_{mn}}=0$:

$$\left(D_2\lambda^2n^3+2D_3m^2n+D_1m^2n\right)\lambda A_{mn}-\frac{(D_1+D_3)\lambda^2mnY_{mn}}{\pi}-\frac{\left(D_2\lambda^3n^2+D_3\lambda m^2+J_y\lambda^3\right)Y_{mn}}{\pi}$$

$$-16\sum_{p=1}^{\infty}\sum_{q=1}^{\infty}\frac{\left(2D_5\lambda^2mn^2pq+D_5\lambda^2mpq^3+D_4mp^3q\right)A_{pq}}{\pi^2M}+16\sum_{p=1}^{\infty}\sum_{q=1}^{\infty}\frac{\left(D_5\lambda^3mn^2q+D_4\lambda mp^2q\right)X_{pq}}{\pi^3M}$$

$$+16\sum_{p=1}^{\infty}\sum_{q=1}^{\infty}\frac{D_5\lambda^2(n^2+q^2)mpY_{pq}}{\pi^3M}=0\tag{9}$$

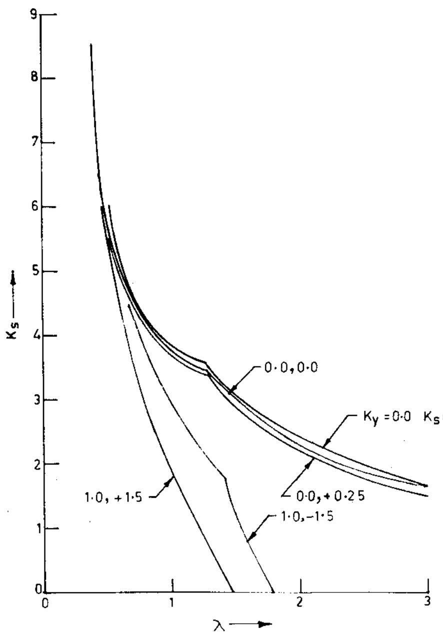

Fig. 2 Variation of k_x with λ ($\theta = 45$ deg, $t_c/t_f = 20$, and $\gamma_x = \gamma_y = 0$).

where

$$D_1 = D_{12}/D_{11} \qquad D_2 = D_{22}/D_{11}$$

$$D_3 = D_{33}/D_{11} \qquad D_4 = D_{13}/D_{11}$$

$$D_5 = D_{23}/D_{11} \qquad J_x = S_x b^2/\pi^2 D_{11}$$

$$J_y = S_y b^2/\pi^2 D_{11} \qquad k_s = N_{xy} b^2/\pi^2 D_{11}$$

$$k_x = N_{0x} b^2/\pi^2 D_{11} \qquad k_y = N_{0y} b^2/\pi^2 D_{11}$$

$$M = (m^2 - p^2)(n^2 - q^2) \qquad X_{mn} = bB_{mn}/S_x$$

$$Y_{mn} = bC_{mn}/S_y \qquad \lambda = a/b \tag{10}$$

In Eqs. (7–10), m, n, p, and q are to be chosen such that $(m \pm p)$ and $(n \pm q)$ are odd integers. N_{0x}, N_{0y}, and N_{xy} are the maximum values of the in-plane forces and γ_x and γ_y the bending load coefficients (Fig. 1a). k_x, k_y, and k_s are, respectively, the nondimensionalised values of N_{0x}, N_{0y}, and N_{xy}.

Numerical Results

The expansion of Eqs. (7–9) for a specified range of values of indices m and n gives a set of $3mn$ homogeneous algebraic equations in A_{mn}, $B_{mn}(X_{mn})$, and $C_{mn}(Y_{mn})$. The buckling coefficient k_x for given values of k_y and k_s can be evaluated from the condition that the determinant of the coefficients of A_{mn}, B_{mn}, and C_{mn} in the resulting equations should be zero for their nontrivial solution. The undetermined coefficients B_{mn} and C_{mn} are eliminated in Eq. (7) by their solution as a result of the recurrance of Eqs. (8) and (9) in terms of A_{mn}. The algebraic equations resulting from Eq. (7) after the elimination of $B_{mn}(X_{mn})$ and $C_{mn}(Y_{mn})$ can be cast into a matrix form as

$$[P]\{A\} = k_x[Q]\{A\} \tag{11}$$

where P and Q are real symmetric matrices and A is a column vector of A_{mn} arranged as

$$A = [A_{11} \quad A_{12} \dots A_{1n} A_{21} A_{22} \dots A_{2n} \quad A_{m1} \quad A_{m2} \dots A_{mn}]^T \tag{12}$$

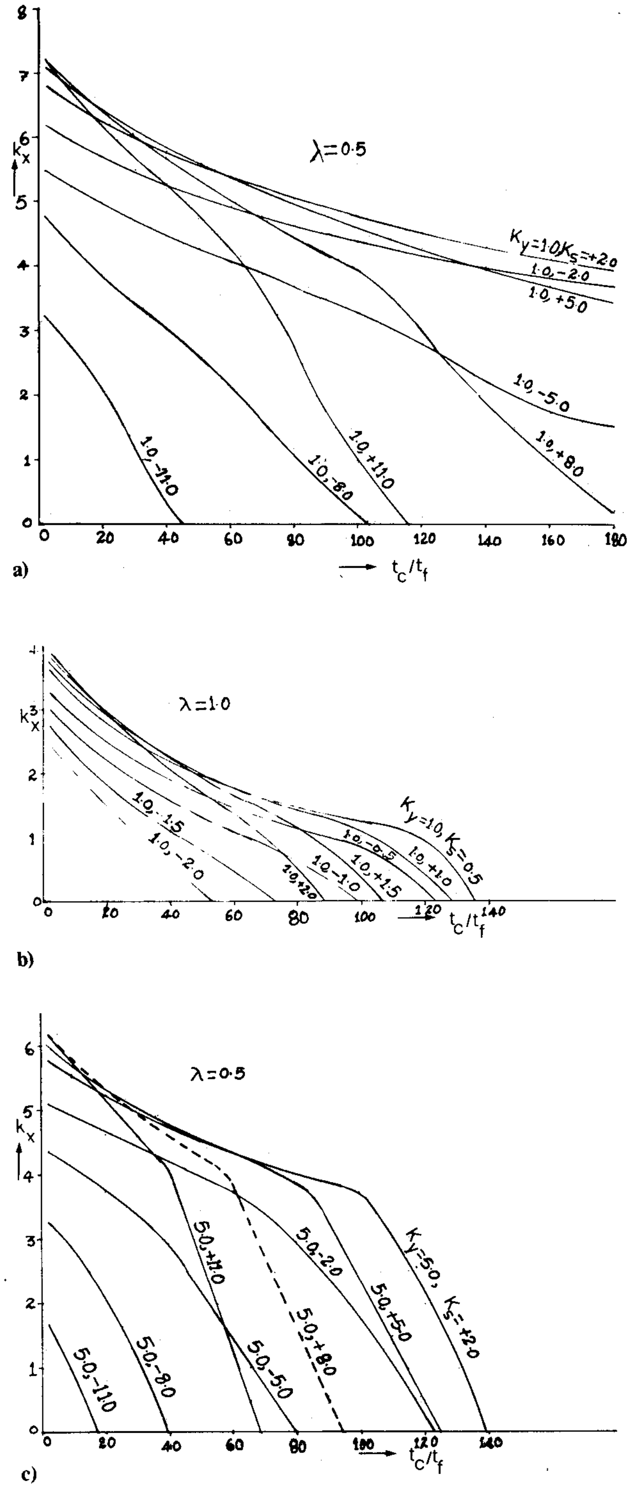

Fig. 3 Variation of k_x with t_c/t_f ($\theta = 45$ deg and $\gamma_x = \gamma_y = 0$).

Table 2 Comparison of present and Ref. 10 results

k_y	k_x (present study)	k_x (Ref. 10, Fig. 8b)	k_s	k_x (present study)	k_x (Ref. 10, Fig. 9b)
0	2.81	2.75	0	2.90	2.82
0.5	2.31	2.29	1.0	2.56	2.50
1.0	1.83	1.79	2.0	2.33	2.28
1.5	1.35	1.31	3.0	1.75	1.71
2.0	0.85	0.83	4.0	0.62	0.59

The matrix P is formed partly by the elasticity of the plate and partly by the in-plane loading associated with normal compression N_y and in-plane shear N_{xy}.

Each face is assumed made of a single layer of a typical glass FRP with the principal material properties of

$$E_1 = 24{,}210 \text{ Pa} \qquad E_2 = 5433 \text{ Pa}$$

$$\mu_{12} = 0.334 \qquad G_{12} = 2452 \text{ Pa}$$

where E_1 and E_2 are, respectively, the longitudinal and transverse elastic moduli, μ_{12} the major Poisson's ratio, and G_{12} the shear modulus. The core is of balsa wood having transverse shear moduli with the specifications

$$G_{xz} = 130 \text{ Pa} \qquad G_{yz} = 10 \text{ Pa}$$

The values of the flexural stiffness D_{11} that will be used to interpret the results are given in Table 1 for different fiber orientation angle θ.

The numerical values of buckling coefficient k_x are evaluated and plotted in Figs 2–7 with varying parameters: aspect ratio λ, core-to-face thickness ratio t_c/t_f, fiber orientation angle θ, bending load coefficient γ_y, and normalized in-plane compression k_y and shear k_s.

The formulation and computerization of the present problem are checked by comparing the results with those of Refs. 8 and 10. When $k_y = k_s = 0$, the values of k_x for a given panel coincide with those of Ref. 8. The stability of corrugated core sandwich plates vs. isotropic faces under combined loading are studied in Ref. 10. For a square plate with isotropic faces, where J_x is equal to infinity and J_y to 2 (i.e., corrugations of the core along the x axis), the buckling coefficient k_x is evaluated by varying k_y and k_s separately. The evaluated results and those obtained from Figs. 8b and 9b of Ref. 10 for $J = 2$ are given in Table 2 for comparison. The solutions are in reasonable agreement.

Discussion

The presence of normal compression k_y and/or shear load k_s reduces the buckling coefficient k_x, as expected. The exception to this observation is the presence of small positive shear (positive shear being as shown in Fig. 1a), which increases the value of the buckling coefficient k_x. See Figs. 2 and 7. The values of k_x at certain values of positive shear are higher than those at numerically equal negative shears k_s, the difference increasing with k_s. See Figs. 2, 3, and 6.

Figure 3 shows that the trends in the variation of k_x with the core-to-face thickness ratio t_c/t_f are different from one graph to the other. Most of the curves at low value of k_y and

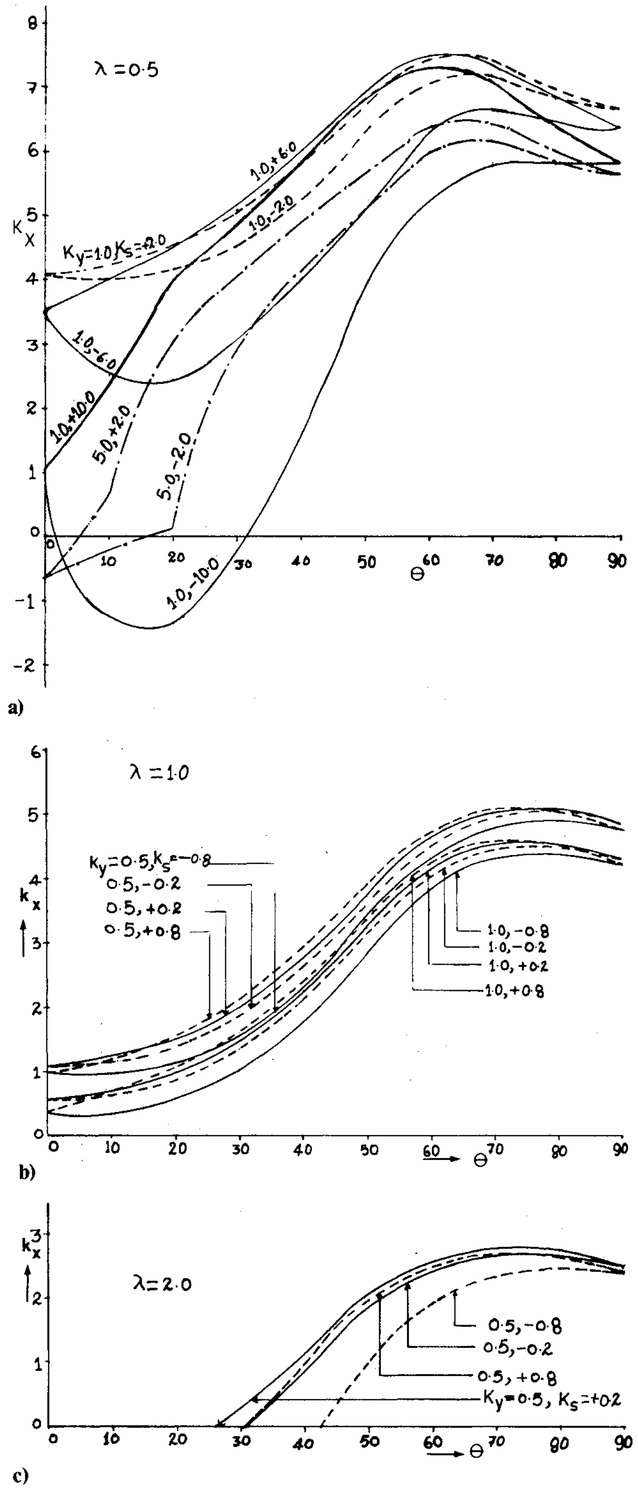

Fig. 4 Variation of k_x with θ ($t_c/t_f = 20$ and $\gamma_x = \gamma_y = 0$).

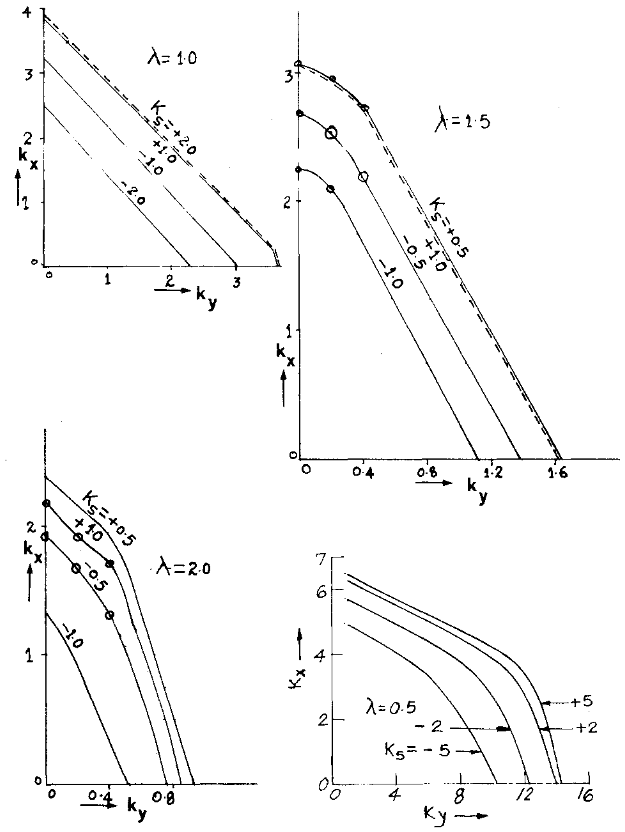

Fig. 5 Variation of k_x with k_y ($\theta = 45$ deg, $t_c/t_f = 20$, and $\gamma_x = \gamma_y = 0$).

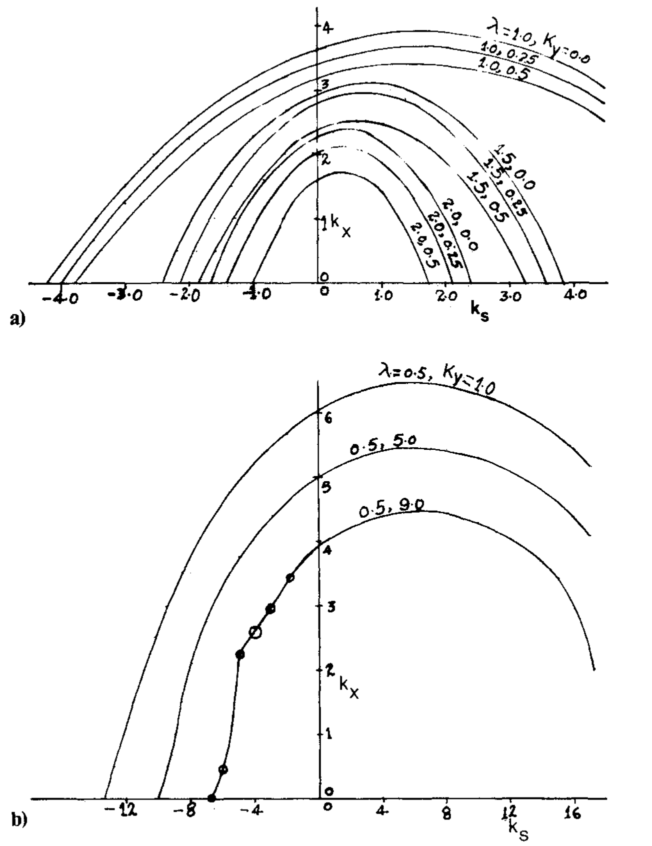

Fig. 6 Variation of k_x with k_s ($\theta = 45$ deg, $t_c/t_f = 20$, and $\gamma_x = \gamma_y = 0$).

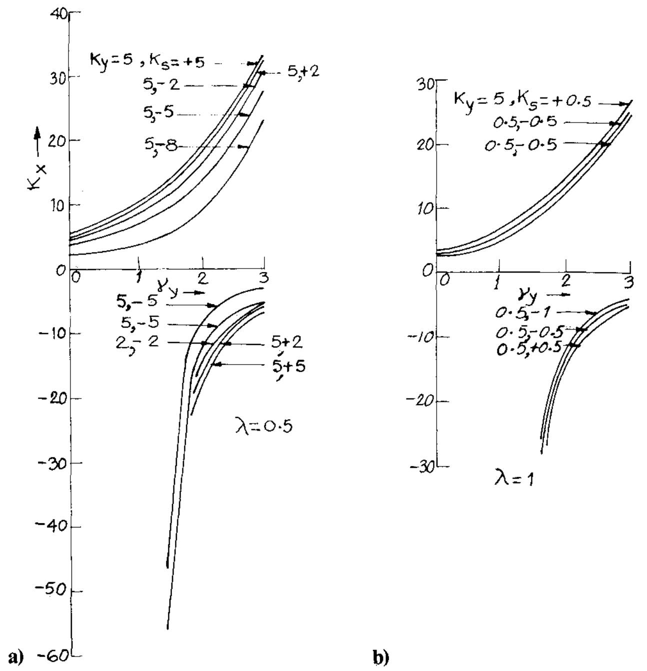

Fig. 7 Variation of k_x with γ_y ($\theta = 45$ deg, $t_c/t_f = 20$, and $\gamma_x = 0$).

Table 3 Values of θ at which buckling load N_{0x} is maximum for various combinations of k_y and k_s

k_y	k_s	θ, deg
1	+10	25
1	−10	65
1	+ 6	15
1	− 6	0
5	+ 2	35
5	− 2	45

k_s (Fig. 3a and 3b) are concave upward, but at high values of k_y and k_s (Fig. 3c) concave downward, i.e., the buckling coefficient k_x decreases rapidly with t_c/t_f at higher values of k_y and k_s. From the upper curves of Fig. 3, one can also observe that, for t_c/t_f less than about 70, k_x is greater at numerically large positive shear than at numerically small negative shear; e.g., k_x at $k_y = 1.0$ and $k_s = +8.0$ is larger than that at $k_y = 1.0$ and $k_s = -2.0$ for $t_c/t_f < 65$. See Fig. 3a.

The interpretation of Fig. 4, which gives the variation of k_x with fiber orientation angle θ for different combinations of k_y, k_s, and aspect ratio λ, is understood better if one converts the nondimensionalized buckling load k_x to its absolute value N_{0x}, using the definition of Eq. (10) and Table 1. At a low aspect ratio, say $\lambda = 0.5$ (Fig. 4a, the buckling load N_{0x} combined with large positive values of k_y and k_s ($k_y = 1$, $k_s = +10$ and $k_y = 5$, $k_s = +2$) increases with θ in the range $0 \leq \theta \leq 90$ deg up to certain values and then starts decreasing. But, in the presence of high negative shear ($k_s = -10$), the buckling load N_{0x} decreases initially, then increases, and again decreases with θ. According to Ref. 8, N_{0x} acting alone (i.e., $k_y = k_s = 0$) continuously decreases with θ for $\lambda = 0.5$. The approximate values of the fiber orientation angle θ at which N_{0x} is maximum for the combinations of k_y and k_s shown in Fig. 4a are listed in Table 3.

In case of the plates having high aspect ratios (say $\lambda = 1$ and 2 in Figs. 4b and 4c), the buckling load N_{0x} rises with θ up to a certain value and then falls. For the combinations of k_y and k_s considered, the value of θ at which N_{0x} is maximum is about 45 deg when $\lambda = 1$ (Fig. 4b) and about 65 deg when $\lambda = 2$ (Fig. 4c).

The variation of k_x with k_y shown in Fig. 5 is bilinear. In the majority of cases, each graph can be split into two portions between which a smooth transition exists; the slope of top portion is less than that of bottom portion, i.e., the buckling coefficient k_x decreases faster over the latter portion. As can be seen from the graphs, the variance in shear load k_s has little influence on these slopes.

The buckling coefficient k_x decreases continuously with increase in negative shear $-k_s$; but k_x increases initially and then decreases with positive shear $+k_s$. See Fig. 6. It is also clear from Fig. 6 that the values of positive shear ($+k_s$) at which k_x is maximum is influenced by the aspect ratio λ; as λ increases, the transition value of k_s decreases. In the cases of isotropic and specially orthotropic sandwich panels, the magnitudes of the positive and negative shear buckling loads coincide and, hence, the graphs of k_x vs k_s are symmetric about $k_s = 0$. The increasing trend of k_x at small values of positive k_s in the case of anisotropic sandwich panels may be attributed to the stiffening of the fibers by tensile forces induced by positive shear; larger values of k_s, however, buckle the plate, thereby decreasing the values of k_x. One can conclude that the presence of smaller positive shear opposes the buckling under compressive force k_x.

The nature of the variation in k_x with the bending load coefficient γ_y in the presence of k_y and k_s (Fig. 7) is similar to that in the absence of the latter (see Fig. 5 of Ref. 8). The influence of γ_y is to increase the buckling coefficient k_x. The numerically smaller value of k_x is negative (i.e., N_{0x} becomes tensile) at higher values of γ_y (say, $\gamma_y > 2$).

Acknowledgment

The material presented here is part of the Postdoctoral work done by the author at the Institute of Light-Weight Structure and Rope Ways, ETH, Zurich, Switzerland.

References

[1]Libove, C. and Batdorf, S.B., "A General Small Deflection Theory for Flat Sandwich Plates," NACA Rept. 899, 1948.

[2]Robinson, J.R., "The Buckling and Bending of Orthotropic Sandwich Panels with All Edges Simply-Supported," *The Aeronautical Quarterly*, Vol. 6, May 1955, pp. 125–148.

[3]Nordby, G.M. and Crisman, W.C., "Strength Properties and Relationships Associated with Various Types of Fiber Glass-Reinforced Facing Sandwich Structures," USAAVLABS Tech. Rep. 65-15, Aug. 1965.

[4]Pearce, T.R.A. and Webber, J.P.H., "Experimental Buckling Loads of Sandwich Panels with Carbon Fibre Face Plates," *The Aeronautical Quarterly*, Vol. 24, Nov. 1973, pp. 295–312.

[5]Gutierrez, A.J. and Webber, J.P.H., "Flexural Wrinkling of Honeycomb Sandwich Beams with Laminated Faces," *International Journal of Solids and Structures*, Vol. 16, No. 7, 1980, pp. 645–651.

[6]Stroud Jr. W.P. and Kingsbury, H.B., "Study of Stresses and Deformations in Sandwich Plates with Anisotropic Facings," *Journal of Aircraft*, Vol. 9, Dec. 1972, pp. 801–802.

[7]Koganti, M.R. and Kaeser, R., "Shear Buckling of Stiff Core Anisotropic Sandwich Plate," *Proceeding of ASCE, Journal of Engineering Mechanics*, Vol. 110, Sept. 1984, pp. 1435–1440.

[8]Koganti, M.R., "Buckling Analysis of FRP Faced Anisotropic Sandwich Plates," *AIAA Journal*, Vol. 23, Aug. 1985, pp. 1247–1253.

[9]Koganti, M.R., "Buckling Analysis of FRP Faced Anisotropic Cylindrical Sandwich Panel," *Proceedings of ASCE, Journal of Engineering Mechanics*, Vol. 111, April 1985, pp. 529–544.

[10]Harris, L.A. and Auelmann, R.R., "Stability of Flat, Simply Supported Corrugated Core Sandwich Plates Under Combined Loads," *Journal of the Aerospace Sciences*, Vol. 27, July 1960, pp. 525–534.

[11]Chang, C.C. and Fang, B.T., "Initially Warped Sandwich Panel Under Combined Loading," *Journal of the Aerospace Sciences*, Vol. 27, Oct. 1960, pp. 779–787.

[12]Kuenzi, E.W., "Buckling Coefficients For Simply Supported Flat Rectangular Sandwich Panels under Biaxial Compression," Forest Products Laboratory, Forest Service, U.S. Dept. of Agriculture, Rept. FPL 135, April 1970.

[13]Jones, R.M., *Mechanics of Composite Materials*, Scripta Book Co., McGraw-Hill, New York, 1975, pp. 45–47.

[14]Pearce, T.R.A. and Webber, J.P.H., "Buckling of Sandwich Panels with Laminated Face Plates," *The Aeronautical Quarterly*, Vol. 23, May 1972, pp. 148–160.